❒   806

Machine learning classifiers for detection of glaucoma

Reshma Verma[1], Lakshmi Shrinivasan[1], Basvaraj Hiremath[2]

[1]Department of Electronics and Communication Engineering, Faculty of ECE, Ramaiah Institute of Technology, Karnataka, India
[2]Department of Medical Electronics, Ramaiah Institute of Technology, Karnataka, India

Article Info	ABSTRACT
	Glaucoma is a disease that affects the optic nerve. This disease, over a period of time, can lead to loss of vision. Which is known as 'silent thief of sight'. There are several methods in which the disease can be treated, if detected at an early stage It is not possible for any technology, including artificial intelligence, to replace a doctor. However, it is possible to develop a model based on several classical image processing algorithms, combined with artificial intelligence that can detect onset of glaucoma based on certain parameters of the retinal fundus. This model would play an important role in early detection of the disease and assist the doctor. The traditional methods to detect glaucoma, as efficient as they may be, are usually expensive, a machine learning approach to diagnose from fundus images and accurately classify its severity can be considered to be efficient. Here we propose support vector machine (SVM) method to segregate, train the models using a high-end graphics processor unit (GPU) and augment the hull convex approach to boost the accuracy of the image processing mechanisms along with distinguishing the different stages of glaucoma. A web application for the screening process has also been adopted.

Corresponding Author:

Reshma Verma
Department of Electronics and Communication Engineering, Ramaiah Institute of Technology
Karnataka, India
Email: reshmaverma@msrit.edu

1. INTRODUCTION

Glaucoma is one of the major causes of blindness, which affects the optic nerves due to the abnormal high pressure in the eye, glaucoma may occur at any age but generally affects older adults. It must be treated at the early stage because the vision loss cannot be regained. An essential pathological characteristic in the progression of glaucoma is the increase in the size of the optic cup with respect to the optic disc. The optic disc, or optic nerve head, is the region in the retina where the optic nerve fibers, or ganglion cells, aggregate to form the optic nerve, which is connected to the brain. Within this optic disc is a depression known as the optic cup.

During glaucomatous progression, the death of the ganglion nerve cells leads to increased excavation of the optic cup, and a corresponding increase in the optic cup to disc ratio (CDR). The CDR is thus a vital indicator of glaucomatous neuropathy as it is indicative of actual pathological changes in the retina during glaucoma. The most common way to detect glaucoma is by finding CDR. Optic disk detection is the foremost thing in developing automated diagnosis systems.

A normal eye has an average CDR of 0.3 to 0.5. The CDR gives us the information about the different stages of glaucoma in an eye. The proposed system utilizes artificial intelligence to detect the presence of glaucoma in a human eye. Glaucoma can be detected by the analysis of CDR. The first part involves to build a machine learning model using a support vector machine (SVM) and K-means classifier and the rest involves building a convolutional neural network for the same.

The use of machine learning models and convolution neural networks present at the backend of the designed web application makes it simpler to detect glaucoma [1]–[3] than the traditional methods which involve manual detection. The proposed autonomous system develops a complete decision support system for early glaucoma detection. Paper [4]–[6] It provides analysis, design, implementation, and testing of novel algorithms for a complete decision support system for glaucoma detection with powerful feature selection strategies, we have also performed extensive experiments to evaluate the performance of the proposed glaucoma detection system on real datasets and comparisons with existing state of the art techniques for performance assessment and provide a screening process which is easy to access to everyone.

2. METHODOLOGY

The overall methodology implemented is shown in Figure 1. The fundus image obtained from optical coherence tomography (OCT) [7] is split into red, green and blue (RGB) channels. Contrast limited adaptive histogram equalization (CLAHE) [8] filter is applied to increase the contrast adaptive to the image as it will make the cup and disc extraction easier. The mean and standard deviation (SD) of the pixel values are obtained. Red channel is used for the extraction of the disc and green channel is used for extraction of the cup, by determining the threshold value from the mean and SD values of the pixels, histogram analysis is done to perform thresholding. Then repeated morphological opening and closing operations are performed to reduce the noise in the image. Convex hull is adopted to join the contours which are found to be more effective. The contours of the obtained binary image are detected. The ellipse is drawn around the largest contour obtained. A bounding rectangle is drawn around the ellipse to obtain the major axis of the ellipse. Similar procedure is followed to obtain the diameter of the cup. TheCDR is obtained by dividing the length of the cup axis by that of the disc axis.
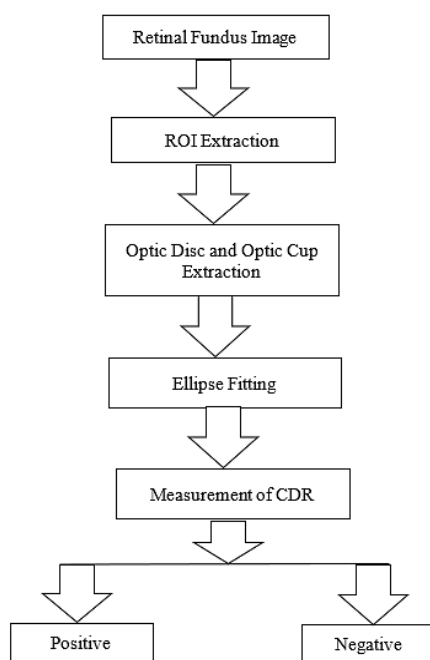

Figure 1. Proposed CDR computing methodology

2.1. Non-adaptive histogram equalization

Histogram equalization normally improves the contrast of the image. Another important feature is that, even if the image was a darker image, after equalization we acquire almost the same image. As a result, this is used as a "reference tool" to make all images with the same lighting condition.

2.1.1. Contrast limited adaptive histogram equalization

The global contrast of the image in histogram equalization [9] in many cases is not considered to be efficient method, due to over-brightness most of the information is lost as histogram is not confined to a particular region, and in order to overcome this issue adaptive histogram equalization is proposed. In this method the image is divided into small blocks called "tiles" then each of these blocks are histogram equalized,

in a small area, histogram would be confined to a small region (unless there is noise). In the presence of noise, it will be amplified. To avoid this, contrast limiting is implemented. If any histogram bin is above the specified contrast limit, those pixels are clipped and distributed uniformly to other bins before applying histogram equalization. After equalization, to remove artifacts in tile borders, bilinear interpolation is implemented.

a.   Thresholding

From a grayscale image, thresholding can be used to create binary images. A threshold value of pixel intensity is chosen and when thresholding [10], [11] is applied all the pixels with values greater than this threshold are turned white and the rest of the pixels are blacked out. The OCT-drishtiGS_033 is depicted in Figure 2. To make the process adaptive to images an adaptive threshold value is computed by multiple trials and errors: the thresholds, T1 and T2 as depicted in Figure 3 and Figure 4 respectively is computed by the (1) and (2),

$$T1=(0.5\times m)-(2\times\sigma G)-(\sigma RI) \tag{1}$$

$$T2=(0.5\times m)+(2\times\sigma G)+(2\times\sigma GI)+(\mu GI) \tag{2}$$

where,
T1 = threshold for segmentation of optic disc
T2 = threshold for segmentation of optic cup
m = size of Gaussian window
σG = standard 25 deviation of Gaussian window
σRI = std dev of the pre-processed red channel
σGI = std dev of the pre-processed green channel
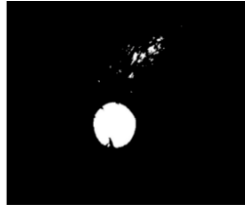μGI = mean of the preprocessed green channel

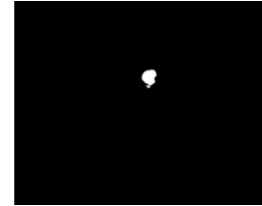Figure 2. OCT image   Figure 3. Segmentation of optic disc   Figure 4. Segmentation of optic cup

b.   Morphological operations and convex hull

Morphological transformations are some simple operations based on the image shape. It is normally performed on binary images. It needs two inputs, one is original image, and the second one is called a structuring element or kernel which decides the nature of operation. Two basic morphological operators are erosion and dilation. Then its variant forms like opening, closing and gradient can also be considered. Opening and closing operation is performed in removal of noise and closing is useful in closing small holes inside the foreground objects as depicted in Figure 5.

In this methodology convex hull using Sklansky algorithm is implemented [12]–[14], given a set of points in the plane, the convex hull of the set is the smallest convex polygon that contains all the points of it. The convex hull of a binary image is the set of pixels included in the smallest convex polygon that surround all white pixels in the input. OpenCV provides us with a convex hull using the Sklansky algorithm. Convex hull is capable of joining nearby contours to form a single contour blob, which might have been broken down because of unwanted noise or disturbance, this algorithm not only successfully joins the contours but also does not alter the size of the original blob unlike other morphological operations [15] as depicted in Figure 6 and Figure 7. Instead of the morphological operations [16], one of the methods adopted to improve the image processing mechanism is the convex hull approach [17] on the thresholded image. The idea is to join nearby contours to form a blob of the size of the optic cup, the methodology adopted is.
−   Define a function to measure distance between the two contours which are passed as its arguments.
−   Define a function which involves nested loops which is used to compare distances between each contour.
−   If the distance is lesser than the threshold defined, a convex hull is used to join the contours, else the smaller contour is ignored.
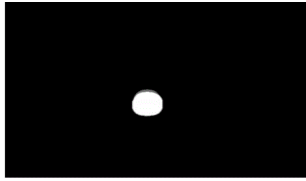
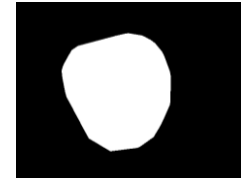Figure 5. Morphological closing

Figure 6. Before convex hull

Figure 7. Contour image after convex hull

c. Contour detection

Contours is a curve joining all the continuous points (along the boundary) as depicted in Figure 8, having the same color or intensity. The contours are a useful tool for shape analysis and object detection and recognition. In OpenCV, finding contours is like finding white object from black background. There are three arguments in cv. findContours () function, first one is source image, second is contour retrieval mode, third is contour approximation method. And it outputs the contours and hierarchy. Contours [18] is a Python list of all the contours in the image. Each individual contour is a Numpy array of (x, y) coordinates of boundary points of the object.

d. Ellipse fitting and bounding rectangle

A bounding rectangle is drawn around the contour. The rectangle is then rotated so that the area is minimum, an ellipse is drawn inside the rotated bounding rectangle joining the midpoints of each side as depicted in Figure 9. The major and minor axis can be obtained as the two sides of the rotated rectangle.
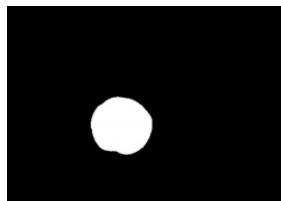

Figure 8. Countour detection

Figure 9. Ellipse fitted for the optic cup

2.2. Design of the classifier

After processing the data, the underlying ground truth of the images are stored in a CSV file. The CDR values of the training set are determined and stored along with its label in a CSV file. The SVM [19] and K-mean clustering [14], [20], [21] classifiers are trained with the training data. The testing data are passed through the classifier to predict the label of the test data for the corresponding CDR values which is calculated for it. The errors in calculation of CDR are determined by subtracting the obtained values from the ground truth values provided by the dataset. The web application architecture developed is depticed in Figure 10. The users by using any of the browsers like Chrome, Mozilla Fox, Opera and Safari, can access the front end of the web application.

Figure 10. Web application architecture

3. RESULTS AND DISCUSSION

3.1. Cup detection

The adopted convex hull approach proved to perform better than the less effective morphological opening and closing [22], [23]. For instance, considering the image drishtiGS_6 as depticed in Figure 11, this has an experimental CDR value of 0.78, as depicted in Figures 11 (a) to 11 (c). The morphological opening generally dilates the image beyond the cup boundary while joining the contours. This generally results in a larger cup to disc ratio than the original, the computation of CDR value is depicted in Figure 12, unlike convex hull as per Figures 12 (a) to 12 (c) the CDR value with convex hull has lower value. Considering another data from drishtiGS_70 as represented in Figure 13, where the original CDR is 0.82 As there was a larger distance between the separated contours, the morphological erosion was having a greater impact than the dilation as depicted in Figures 13 (a) to 13 (c). Figure 14 shows the comparison of the CDR values when these small contours were removed upon repeated erosion. This resulted in a smaller CDR [24]–[26] than expected as depicted in Figures 14 (a) to 14 (c).
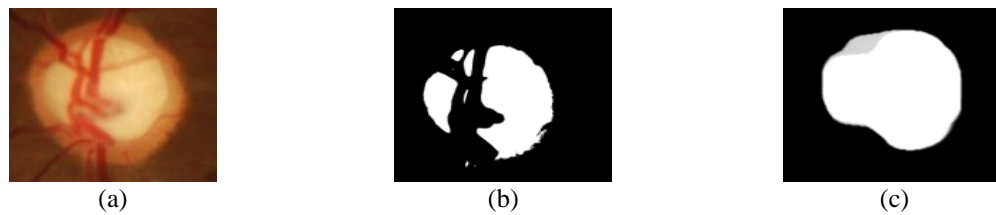

Figure 11. Image of an eye; (a) region of interest, (b) threshold cup, and (c) cup after repeated opening and closing
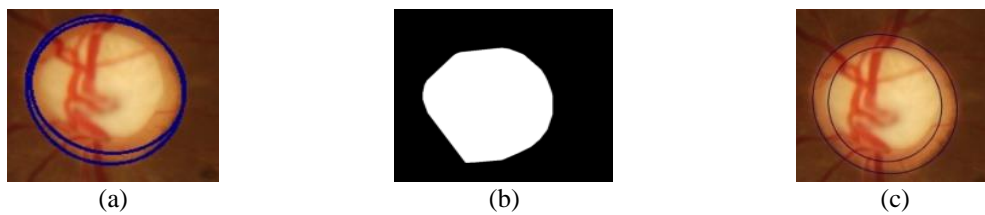

Figure 12. Cup to disc ratio detection; (a) cup and disc detected with repeated morphology CDR: 0.89, (b) cup contours joined after convex hull, and (c) cup and disc detected with convex hull, CDR: 0.8
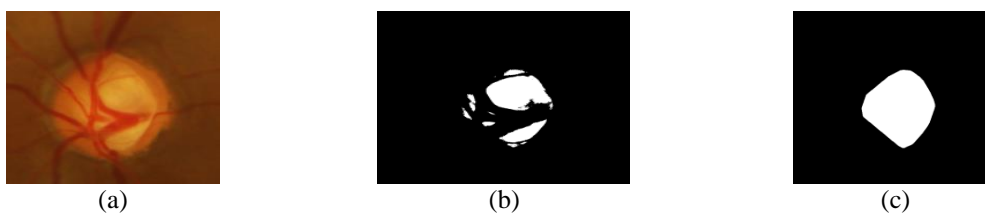

Figure 13. Image of an eye; (a) region of Interest, (b) threshold Cup, and (c) cup after repeated opening and closing
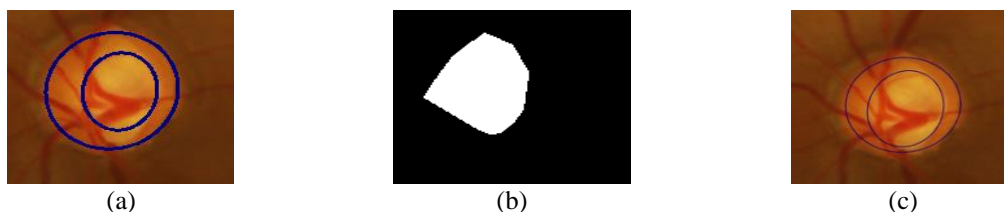

Figure 14. Comparision of CDR values; (a) cup and disc detected with repeated morphology, CDR: 0.69, (b) cup contours joined after convex hull, and (c) cup and disc detected with convex hull, CDR: 0.78

3.2. Disc detection

On observing an image of an eye as represented in Figure 15, it can be noticed that the diameter of the ellipse fitted onto the disc contour remains unchanged. However, the inside noise is cleared which does not really contribute to the CDR as per Figures 15 (a) to 15 (c). Thus, keeping time constraints in mind we can skip the convex hull on the disc, however it is a robust but a time-consuming method with time complexity O (n squared), where n is the number of contours in the thresholded image.

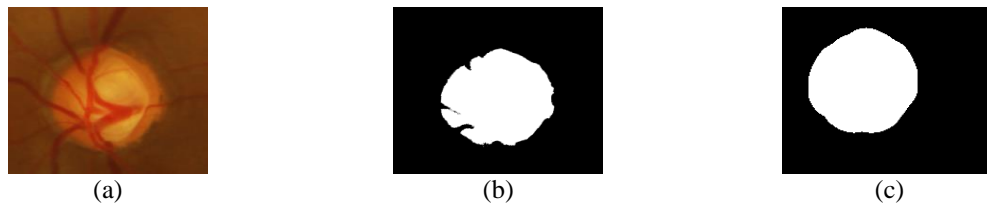(a)   (b)   (c)

Figure 15. Image of an eye; (a) region of interest, (b) disc with repeated morphology, and (c) disc with convex hull

3.3. Calculation of CDR, mean errors and standard deviation

The CDR values calculated from the model are compared with the ground truth values provided by the dataset. The dataset provides CDR values found from four different experiments. The difference between the obtained CDR values with each of those experiments is taken and then the average and the standard deviation of errors of all the images are calculated. The CDR values for each image is calculated. The images are shuffled to training and test data set, and CDR for both are calculated and compared to the four values by the experts which Drishti dataset has been considered. When the values are averaged, the standard deviation and mean errors are obtained. The CDR values of the training and the test images were calculated and stored in two separate CSV files. The CDR values of the training set along with the labels in the ground truth were used to train the model. The CDR values of the test image were passed through the model and the predicted labels were matched with the labels in ground truth. The SVM classifier [27]–[29] was used first and an accuracy of 0.8539 was obtained.

Then the same pair of CDR values of the training set and its labels were passed through the K-means [24]–[26] classifier with K=2 i.e. 2 clusters representing glaucoma and non-glaucoma sets. When the CDR values of the test data were passed through the same an accuracy of 0.7077 was obtained as depicted in Table 1. The model thus proved to have performed better when it was supervised; the Drishti dataset has provided us complete details on each of the 100 images which serve well for supervised learning. The above accuracies are obtained for a 2-dimensional classifier. The web application developed is dependent on the logical relations based on the CDR values obtained after processing the images. After entering the local address in the address bar of a search engine i.e., the homepage displays as depicted in Figure 16, upload the OCT obtained from the hospital through tomography. The website prompts users to enter patient details. Upon submitting, the report is displayed as represented in Figure 17, with the OCT features and report summary stating whether the patient has glaucoma.

Table 1 Accuracies of SVM and K-mean

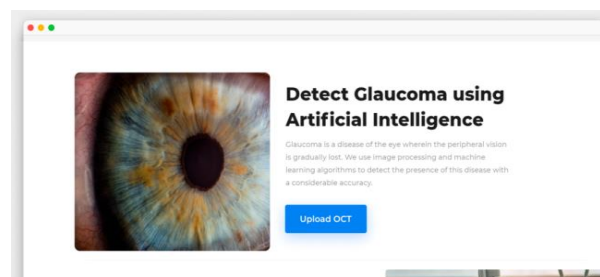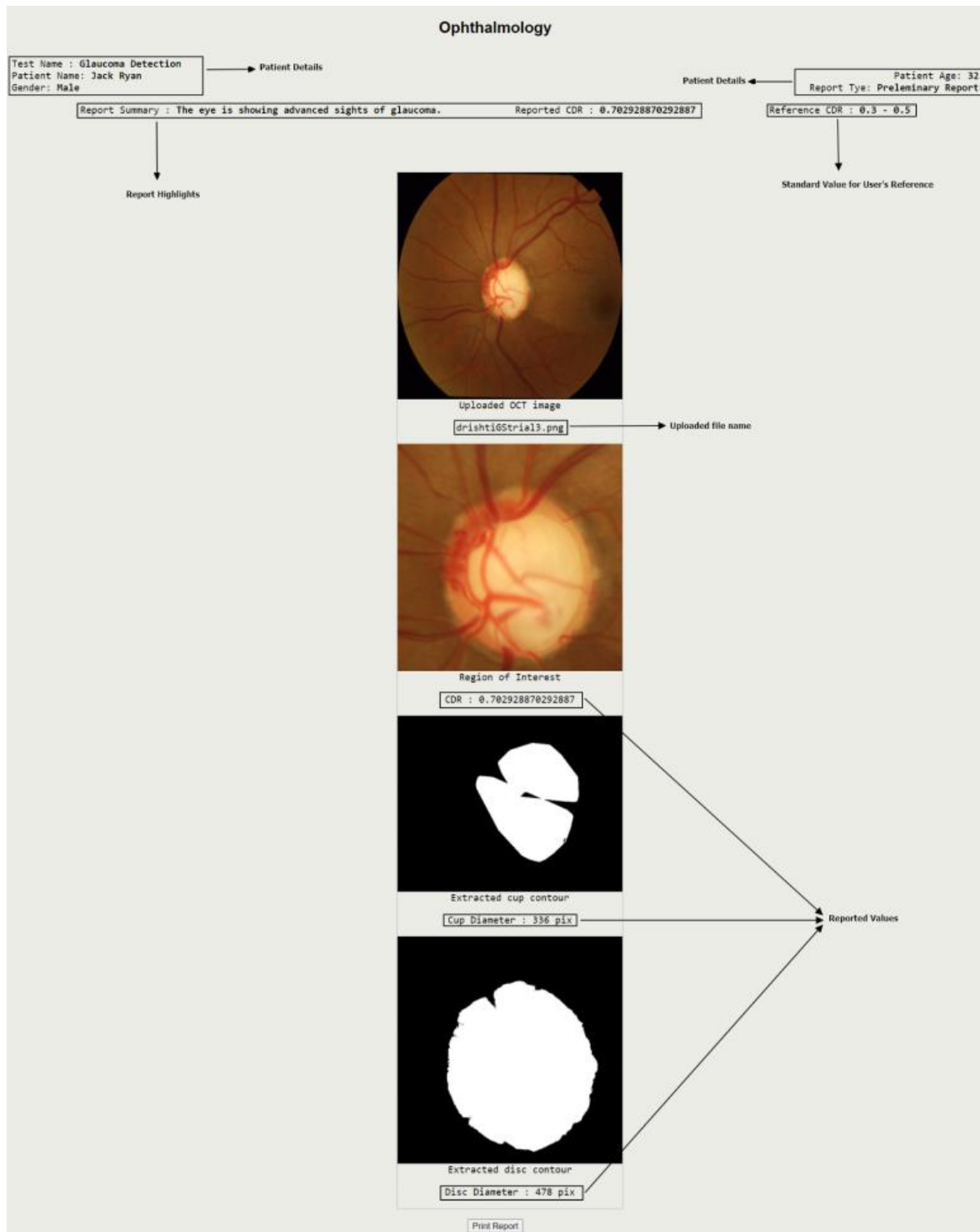| Classifier	SVM	K-means
Accuracy	85.39%	70.77%

Figure 16. Homepage

Figure 17. Patient report

4.   CONCLUSION AND FUTURE SCOPE

The methodology implemented has the comparsion of the performance of SVM against a K-mean clustering algorithm from the CDR obtained using the individual methods. SVM proved to provide better accuracy when compared to K-mean clustering. Furthermore, the result implies lesser error range for the SVM method thus ensuring a better consistency of CDR determination. Convex hull approach was used to diagnose from the fundus image and classify it accurately. Thus, the severity of glaucoma is identified and detection is done at a very early stage. An alternate inexpensive and user-friendly web application is designed and

developed for the screening process. In spite of being a cheap and effective way to detect glaucoma, there is always scope for improvement. One such drawback might be the slow working of the convex hull algorithm used to join contours. The application and the algorithms used to develop it are dependent on the OCT images which are photographed using well trained professionals and making use of tomography equipment available in the hospitals. By making use of proper lenses (preferably a concave) native camera it is still possible to click a photograph of the optic disc. However, the clarity and the precision of the photos might be off the mark, which requires a much robust method for processing such images to obtain the optic disc and cup.

REFERENCES

[1]   L. Divya and J. Jacob, "Performance analysis of glaucoma detection approaches from fundus images," *Procedia Computer Science*, vol. 143, pp. 544–551, 2018, doi: 10.1016/j.procs.2018.10.429.
[2]   C. Zhu *et al.*, "Retinal vessel segmentation in colour fundus images using extreme learning machine," *Computerized Medical Imaging and Graphics*, vol. 55, pp. 68–77, 2017, doi: 10.1016/j.compmedimag.2016.05.004.
[3]   S. Oh, Y. Park, K. J. Cho, and S. J. Kim, "Explainable machine learning model for glaucoma diagnosis and its interpretation," *Diagnostics*, vol. 11, no. 3, 2021, doi: 10.3390/diagnostics11030510.
[4]   N. Mojab, V. Noroozi, P. S. Yu, and J. A. Hallak, "Deep multi-task learning for interpretable glaucoma detection," in *Proceedings - 2019 IEEE 20th International Conference on Information Reuse and Integration for Data Science, IRI 2019*, 2019, pp. 167–174, doi: 10.1109/IRI.2019.00037.
[5]   A. Issac, M. Partha Sarathi, and M. K. Dutta, "An adaptive threshold based image processing technique for improved glaucoma detection and classification," *Computer Methods and Programs in Biomedicine*, vol. 122, no. 2, pp. 229–244, 2015, doi: 10.1016/j.cmpb.2015.08.002.
[6]   C. Raja and N. Gangatharan, "A hybrid swarm algorithm for optimizing glaucoma diagnosis," *Computers in Biology and Medicine*, vol. 63, pp. 196–207, 2015, doi: 10.1016/j.compbiomed.2015.05.018.
[7]   G. An *et al.*, "Glaucoma diagnosis with machine learning based on optical coherence tomography and color fundus images," *Journal of Healthcare Engineering*, vol. 2019, 2019, doi: 10.1155/2019/4061313.
[8]   S. Masood, M. Sharif, M. Raza, M. Yasmin, M. Iqbal, and M. Javed, "Glaucoma disease: a survey," *Current Medical Imaging Reviews*, vol. 11, no. 4, pp. 272–283, 2015, doi: 10.2174/1573405611104150727171246.
[9]   A. Latif *et al.*, "Content-based image retrieval and feature extraction: a comprehensive review," *Mathematical Problems in Engineering*, vol. 2019, 2019, doi: 10.1155/2019/9658350.
[10]   A. Sarhan, J. Rokne, and R. Alhajj, "Glaucoma detection using image processing techniques: a literature review," *Computerized Medical Imaging and Graphics*, vol. 78, 2019, doi: 10.1016/j.compmedimag.2019.101657.
[11]   A. Agarwal, S. Gulia, S. Chaudhary, M. K. Dutta, R. Burget, and K. Riha, "Automatic glaucoma detection using adaptive threshold based technique in fundus image," in *2015 38th International Conference on Telecommunications and Signal Processing, TSP 2015*, 2015, pp. 416–420, doi: 10.1109/TSP.2015.7296295.
[12]   T. Kersey, C. I. Clement, P. Bloom, and M. F. Cordeiro, "New trends in glaucoma risk, diagnosis and management," *Indian Journal of Medical Research*, vol. 137, no. 4, pp. 659–668, 2013.
[13]   A. Poshtyar, J. Shanbehzadeh, and H. Ahmadieh, "Automatic measurement of cup to disc ratio for diagnosis of glaucoma on retinal fundus images," in *Proceedings of the 2013 6th International Conference on Biomedical Engineering and Informatics, BMEI 2013*, 2013, pp. 24–27, doi: 10.1109/BMEI.2013.6746900.
[14]   G. Babu.T.R, R. Sathishkumar, and R. Venkatesh, "Segmentation of optic nerve head for glaucoma detection using fundus images," *Biomedical and Pharmacology Journal*, vol. 7, no. 2, pp. 697–705, Dec. 2014, doi: 10.13005/bpj/544.
[15]   Z. Ghassabi, J. Shanbehzadeh, and K. Nouri-Mahdavi, "A unified optic nerve head and optic cup segmentation using unsupervised neural networks for glaucoma screening," in *Conference proceedings : Annual International Conference of the IEEE Engineering in Medicine and Biology Society. IEEE Engineering in Medicine and Biology Society. Annual Conference*, 2018, vol. 2018, pp. 5942–5945, doi: 10.1109/EMBC.2018.8513573.
[16]   J. Cheng *et al.*, "Superpixel classification based optic disc and optic cup segmentation for glaucoma screening," *IEEE Transactions on Medical Imaging*, vol. 32, no. 6, pp. 1019–1032, 2013, doi: 10.1109/TMI.2013.2247770.
[17]   M. Saravanan, B. Kalaivani, and R. Geethamani, "Glaucoma detection and its classification using fuzzy-C means and K-means segmentation," *International Journal Engineering Research in Computer Science and Engineering (IJERCSE)*, vol. 5, no. 3, pp. 147–151, 2018.
[18]   V. Kamat, S. Chatti, A. Rodrigues, C. Shetty, and A. Vadji, "Glaucoma detection using enhanced k-strange points clustering algorithm and classification," *IOSR Journal of Computer Engineering*, vol. 19, no. 04, pp. 44–49, 2017, doi: 10.9790/0661-1904014449.
[19]   Y. Yao *et al.*, "K-SVM: an effective SVM algorithm based on K-means clustering," *Journal of Computers (Finland)*, vol. 8, no. 10, pp. 2632–2639, 2013, doi: 10.4304/jcp.8.10.2632-2639.
[20]   Q. Abbas, "Glaucoma-deep: detection of glaucoma eye disease on retinal fundus images using deep learning," *International Journal of Advanced Computer Science and Applications*, vol. 8, no. 6, 2017, doi: 10.14569/ijacsa.2017.080606.
[21]   A. Chakravarty and J. Sivaswamy, "Glaucoma classification with a fusion of segmentation and image-based features," in *Proceedings - International Symposium on Biomedical Imaging*, 2016, vol. 2016-June, pp. 689–692, doi: 10.1109/ISBI.2016.7493360.
[22]   S. Xiaoyang, S. Keou, and C. Yazhu, "A computer-based diagnosis system for early glaucoma screening," in *Annual International Conference of the IEEE Engineering in Medicine and Biology - Proceedings*, 2005, vol. 7 VOLS, pp. 6608–6611, doi: 10.1109/iembs.2005.1616016.
[23]   T. Walter and J.-C. Klein, "Automatic analysis of color fundus photographs and its application to the diagnosis of diabetic retinopathy," *Handbook of Biomedical Image Analysis*, pp. 315–368, 2007, doi: 10.1007/0-306-48606-7_7.
[24]   K. Narasimhan and K. Vijayarekha, "An efficient automated system for glaucoma detection using fundus image," *Journal of Theoretical and Applied Information Technology*, vol. 33, no. 1, pp. 104–110, 2011.
[25]   P. K. Suryawanshi, "An approach to glaucoma using image segmentation techniques," *International journal of engineering schiences and research technology*, vol. 2, no. 9, 2013.
[26]   A. Pachiyappan, U. N. Das, T. V. Murthy, and T. Rao, "Automated diagnosis of diabetic retinopathy and glaucoma using fundus and OCT images," *Lipids in Health and Disease*, vol. 11, 2012, doi: 10.1186/1476-511X-11-73.

[27] T. Johnson and S. K. Singh, "Enhanced K strange points clustering algorithm," in *Proceedings - 2015 2nd International Conference on Emerging Information Technology and Engineering Solutions, EITES 2015*, 2015, pp. 32–37, doi: 10.1109/EITES.2015.14.

[28] K. Choudhary and S. Tiwari, "ANN glaucoma detection using cup-to-disk ratio and neuroretinal rim," *International Journal of Computer Applications*, vol. 111, no. 11, pp. 8–14, 2015, doi: 10.5120/19581-1233.

[29] R. Burman, A. Almazroa, K. Raahemifar, and V. Lakshminarayanan, "Automated detection of optic disc in fundus images," *Springer Proceedings in Physics*, vol. 166, no. 1, pp. 327–334, 2015, doi: 10.1007/978-81-322-2367-2_41.

BIOGRAPHIES OF AUTHORS

Dr Reshma Verma received the Ph.D. degree from Jain University, India in 2018. Currently she is working as Assistant Professor in the Department of ECE, Ramaiah Institute of Technology, Karnataka, India. Her research interest is artificial intelligence, image processing and embedded system design. She has published several National, International conferences and indexed journals. She has guided several PG and UG projects. She can be contacted at email: reshmaverma@msrit.edu.

Dr Lakshmi Shrinivasan holds a Ph.D. degree from Jain University, India in 2018. She also received her B.E. from Maharashtra and M.Tech. (Electronics) from VTU, Karnataka, India in 1999 and 2007, respectively. She is currently working as an Associate professor in Dept of ECE at Ramaiah Institute of Technology, Bangalore. Her research interests are artificial intelligence, embedded system. She can be contacted at email: Lakshmi.s@msrit.edu.

Dr. Basavaraj Hiremath received Ph.D. degree from Jain University, India in 2018. Currently he is working as Assistant Professor in the Department of Medical Electronics Engineering, Ramaiah Institute of Technology, Karnataka, India. His research intrest in medical image processing, biomedical signal processing, artificial Intelligence and embedded system design. He has published several National, International conferences and indexed journals. He has 20 years of academic and 1 year of Industry experience. He has guided several PG and UG projects. He can be contacted at email: bvhiremath@msrit.edu.